

# Body Temperature Regulation via Neurotransmitter Control

Tangran (Tony) Dong, Jacqueline Fontanares, Jirach (Jinn) Kungsamut, You-cheng (Darian) Lin, Esmeralda Lopez

Department of Bioengineering, University of California, San Diego

**Abstract**— Our knowledge of the sweating mechanism in thermoregulation was applied to a control system using simulink. Specifically, the focus was on the body's ability to release the neurotransmitter acetylcholine which in turn initiates the sweating mechanism that is capable of cooling the body temperature when it rises above the target level. The application of this physiological mechanism to a control system was successful in that the simulink results indeed supported the correlation between the rise of acetylcholine concentration in the body when the body temperature is above target level. Additionally, there was a decrease in acetylcholine concentration and body temperature over time. The system proved to be effective in cooling the body back down to ideal temperature from a hyperthermic temperature as evidenced by a series of figures over time, furthermore its stability was quantified and confirmed through the use of bode plots. While one bode plot reflected an unstable system at steady state, the incorporation of PID control in the system yielded a bode plot that reflected a stable, single order system. Simplifications and assumptions in the system design made its success in replicating the sweating mechanism in a hyperthermic body achievable, however they also made the system much less realistic to the true physiology of sweating and thermoregulation.

**Keywords** — Thermoregulation; Neurotransmitter; Control System; Hyperthermia.

## I. INTRODUCTION

### A. Background and Motivation

While there are several methods the body utilizes to thermoregulate such as metabolic control and vasodilation, this system design focuses on the sweating mechanism that takes place in the sympathetic nervous system [1]. The rise of body temperature above a target normal body temperature of 310.15K results in the hypothalamus releasing acetylcholine via electrical nerve impulses. Acetylcholine is a neurotransmitter that is released by the sympathetic nervous system on the sweat glands. Sodium, chlorine, and water proceed to exit the body through the sweat glands. As a result, body temperature is regulated; this is an example of a negative feedback loop where the body sweats in order to lower the temperature when it rises above the target level. Fig. 1 below is a visual that better depicts this feedback loop [2].

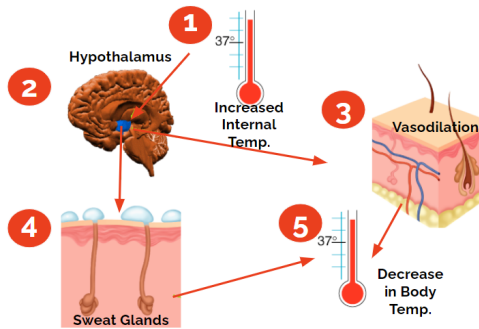


Fig. 1. Physiology of Body Temperature Regulation [2].

Here it is clear that as the temperature increases, an impulse goes through the hypothalamus which then causes vasodilation and sweating to occur. As a result, the body temperature decreases in an effort to maintain body temperature homeostasis.

Hyperthermia occurs when the body temperature rises above 312.55K, which then causes concerns for heat stroke,

sepsis, and impaired circulation [3]. Overheating is a serious concern as there were 10,527 deaths between 2008 and 2014 correlated to cardiovascular, endocrine, and metabolic disorders [4].

This control system is designed to further display and analyze the correlation between acetylcholine concentrations and thermoregulation of the body under hyperthermic conditions in the effort to contribute to the research that might aid in the realm of thermoregulation.

### B. Specific Aims

The small temperature change as a result of acetylcholine inducing the sweating process is a measurable quantity. The goal of this paper is to model the relationship between this temperature change and acetylcholine concentration while the body is under hyperthermic conditions. In this scenario, the body starts at a high initial temperature of 312.55 K (or 40°C) and settles at a final temperature of 310.15 K (or 37°C), which is considered normal body temperature. To make the system ideal, the control aspects of the model were made to limit oscillations and maintain stability according to its phase margin, both of which were tested by creating bode plots.

## II. METHODS

### A. Defining the System

The control system models thermoregulation in hyperthermia by assuming sweating is the only method the body uses to lower its temperature. In this simplified model, we considered acetylcholine as the primary hormone that regulates the sweating rate. The biosystem incorporates heat production via metabolism and heat loss due to sweating and the evaporation of water. The temperature difference between the environment and the body is also considered in the system. To estimate the heat loss from sweating and evaporation, we apply the heat transfer coefficient of the body and the evaporation heat of water. In addition to the biosystem, a PID controller was implemented to adjust the secretion rate of acetylcholine, as the temperature changes and therefore sweat rate and acetylcholine release rate change as well.

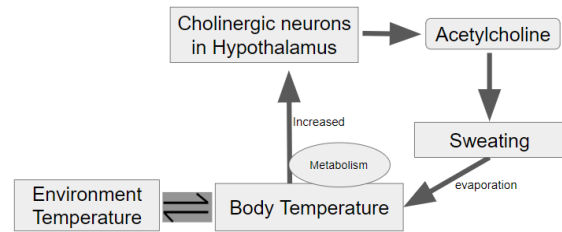


Fig. 2. Simplified block diagram of thermoregulation in hyperthermia when sweating is the only mechanism to reduce heat

### B. Assumptions and Limitations

The first assumption is that the boundary for the system is defined as the skin, and the initial body temperature is 40 degrees, which is in a hyperthermia state compared to our targeted temperature of 37 degrees. Second, we assumed a body mass index of 70 kilograms as the average body weight. Two other important assumptions in our model are that we select sweating as the only mechanism to reduce the body

temperature and that acetylcholine is the only neurotransmitter to trigger sweating. Last, we modeled the heat lost due to the difference between body temperature and the environment temperature as a simple heat exchange equation. As a result, we can calculate total body heat loss as metabolic heat minus heat loss due to temperature differences and sweating.

The scope of the project was limited by these assumptions made. This model assumes parameters relating to an “average body” and therefore parameters such as mass and area would need to be adjusted for different people. Additionally, every person reacts to acetylcholine differently and so the model is limited by the governing equations, which assumes perfect conversion of acetylcholine to induce sweat rate, which may not be accurate to a specific person. Another limitation is that the model assumes there is no active movement, which would vary metabolic rate, but the model assumes constant metabolic rate. The system also is limited by it not including other cooling processes, such as vasodilation, which in addition to cooling the body faster may also affect the rate at which acetylcholine reaches the sweat glands.

### C. Governing Equations

For the sake of a simplified control system, the factors considered in the process of thermoregulation are limited to heat production due to metabolism, heat loss from sweat, and heat transfer with the environment due to ambient temperature gradients. Our simplified model for thermoregulation has been represented with the following governing equations.

$$\frac{dT_{body}}{dt} = \frac{1}{mc_{body}} (M_{rate} - Q_{rate} + k(T_{env} - T_{body}(t))) \quad (1)$$

$$Q_{rate} = S_{rate} \cdot H_{water} \quad (2)$$

$$S_{rate} = (fe^{gC(t)} + h) \cdot U \quad (3)$$

$$U = 10,000 \frac{cm^2}{m^2} \times \frac{1 kg}{1,000,000 mg} \times A \times \frac{1 min}{60 sec}$$

$$\frac{dC}{dt} = \alpha I(t) - \frac{1}{\tau} C(t) \quad (4)$$

Equation (1) represents the change in body temperature as a function of metabolic heat production ( $M_{rate}$ ), heat loss due to sweating ( $Q_{rate}$ ), and the body’s core temperature ( $T_{body}$ ). This equation is derived from specific heat.

$$Q = mc\Delta T \rightarrow dT = \frac{1}{mc} dQ \rightarrow \frac{dT}{dt} = \frac{1}{mc} \frac{dQ}{dt}$$

$$\frac{dQ}{dt} = M_{rate} - Q_{rate} + k(T_{env} - T_{body}(t))$$

From the specific heat formula, the mass (m) and specific heat capacity ( $C_{body}$ ) were constants, described as the mass and specific heat capacity of an average adult body. In this model,  $M_{rate}$  was also a constant and was defined as the product of an average adult’s metabolic rate and body surface area. The heat transfer rate (k) was given by the product of the heat transfer coefficient of a body and the body surface area, and was used as a coefficient for multiplying the third term of  $\frac{dQ}{dt}$ , the temperature gradient term. In this third term, the environmental temperature ( $T_{env}$ ) was assumed to be 40 °C to simulate high ambient temperatures.

TABLE 1. MODEL CONSTANTS

Parameter	Value	Parameter	Value
<b>m</b>	70 kg	<b>a<sup>[4]</sup></b>	200 m <sup>-3</sup>
<b>C<sub>body</sub><sup>[1]</sup></b>	2980 J/(kg·K)	<b>τ<sup>[5]</sup></b>	0.0855 s <sup>-1</sup>
<b>M<sub>rate</sub><sup>[2]</sup></b>	102 W	<b>A<sup>[6]</sup></b>	1.7 m <sup>2</sup>
<b>k<sup>[3]</sup></b>	7.99 W/K	<b>f</b>	-0.8585
<b>T<sub>env</sub></b>	313.15 K	<b>g</b>	-0.05563
<b>H<sub>water</sub></b>	58.1 × 10 <sup>6</sup> J/kg	<b>h</b>	0.9023

Equation (2) represents the heat loss due to sweating as the product of the sweat rate ( $S_{rate}$ ) and the constant evaporation heat of water ( $H_{water}$ ), assuming uniform coverage of the body. Equation (3) represents the sweat rate, and was determined through exponential curve fitting of published data on the relationship between sweat rate and acetylcholine, with the fitting model following the basic form  $y = ae^{-bx} + c$ . The coefficients a, b, and c were determined within 95% confidence bounds. The external terms to the right of the equation are simply unit conversions to g/s, with a constant (U) representing these unit conversions. This equation was therefore a function of the acetylcholine concentration.

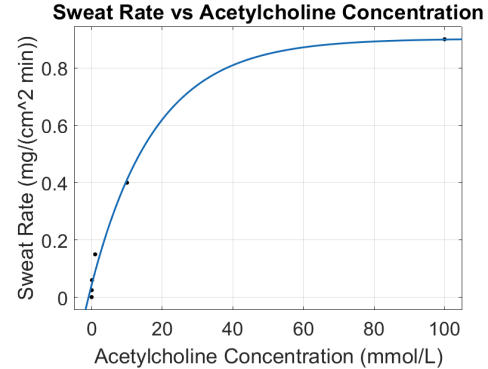


Fig. 3. Exponential curve fitting of sweat rate vs acetylcholine data

The change in acetylcholine concentration is described by (4), which is modeled as a linear ODE. This ODE serves as part of the feedback mechanism in the control system, and consists of the secretion rate ( $I(t)$ ) and the concentration ( $C(t)$ ) of acetylcholine. The constants  $\alpha$  and  $\frac{1}{\tau}$  are defined as  $\frac{1}{blood\ volume}$  and the blood flow rate, respectively, and are the coefficients of this ODE.  $I(t)$  serves as the PID control for this system, with coefficients  $k_p$ ,  $k_i$ , and  $k_d$ , with a target value ( $T_{target}$ ) of 37 °C to simulate body temperature. For this model specifically, PD control is used to cancel out a pole in the biosystem, resulting in a first order system with low pass filter behavior. Derivative control also reduces oscillations in the system response.

$$I(t) = k_p e(t) + k_i \int_{-\infty}^t e(t)dt + k_d \frac{d}{dt} e(t)$$

$$e(t) = T_{body}(t) - T_{target}$$

TABLE 2. CONTROL SYSTEM PARAMETERS

Parameter	Value
<b>k<sub>p</sub></b>	0.0156
<b>k<sub>i</sub></b>	0
<b>k<sub>d</sub></b>	0.9336
<b>C<sub>initial</sub></b>	0 mmol/L
<b>T<sub>body,initial</sub></b>	313.15 K
<b>T<sub>target</sub></b>	310.15 K

### D. Laplace Transform and Linearization

While the governing equations above are more realistic of the acetylcholine and sweat rate system, (1) is nonlinear and therefore more difficult to model. In order to find the transfer function, the biosystem was linearized around a steady state temperature of 37°C and acetylcholine concentration of 0 mmol/L. As a result, the modeled system may only be accurate for small changes around the steady state, represented by  $T_{\sim}$  and  $C_{\sim}$  respectively.

$$\frac{dT_{linear}}{dt} = \frac{-k}{mC_{body}} \tilde{T} - \frac{H_{water}fgA}{6000mC_{body}} \tilde{C} \quad (5)$$

Using (4) and (5), the transfer function for the biosystem,  $B(s)$ , as a rate of temperature to the rate of acetylcholine entering the system was found using Laplace transformations. The resulting biosystem transfer equation was:

$$B(s) = \frac{d\tilde{T}}{d\tilde{I}} = \left( \frac{-H_{water}fgA\alpha}{6000mC_{body}} \right) \times \frac{1}{s + \frac{1}{\tau}} \times \frac{1}{s + \frac{k}{mC_{body}}} \quad (6)$$

Here, the first term is made entirely of constants and determines the amplitude of the system. The next two terms reveal poles of the system. These parts of the system can be defined as:

TABLE III. TRANSFER FUNCTION PARAMETERS

<i>Amp</i>	$\frac{-H_{water}fgA\alpha}{6000mC_{body}}$
$p_1$	$\frac{1}{\tau}$
$p_2$	$\frac{k}{mC_{body}}$

And so the transfer function can then be written in terms of its poles, as seen in (7). Further, the resulting control loop, including both the biosystem and PD controller (explained in detail in the next section) was calculated, seen in (8). Both parts of the loop are shown below in the block diagram (Fig. 4), where the PID controller  $G(s)$  primarily influences the input rate of acetylcholine in (4). Note that there was no measurement error implemented since the measurement is assumed to be accurate and instantaneous, as the model assumes the process takes place over several hours compared to a small delay.

$$B(s) = Amp \times \frac{1}{s^2 + (p_1 + p_2)s + (p_1 p_2)} \quad (7)$$

$$OL(s) = \frac{Amp \times (K_d s + K_p)}{s^2 + (p_1 + p_2)s + (p_1 p_2)} \quad (8)$$

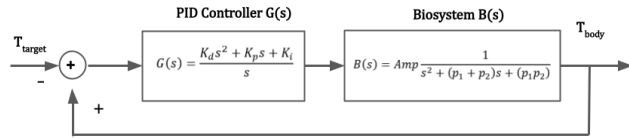


Fig 4. Block Diagram of the temperature system

#### E. Simulink Block Diagram

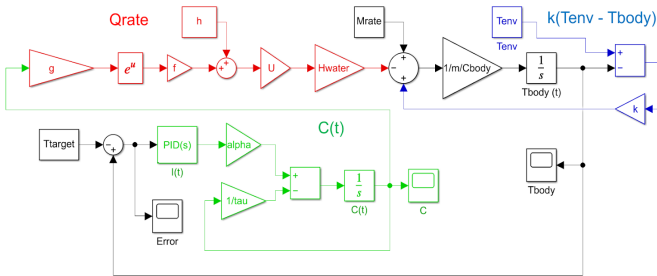


Fig. 5. Simulink Model for the biosystem.

The Simulink model was constructed based on the two governing equations (1) and (4), and the block diagram (Fig. 2). Note that the sign of the summation block was opposite

from regular feedback control because an increase in acetylcholine secretion would decrease body temperature rather than increase it.

#### F. Sensitivity and Bode Analysis

The open loop transfer function without PID control was previously obtained by Laplace transform (7). The transfer function was plugged into MATLAB to graph the open loop Bode plot.

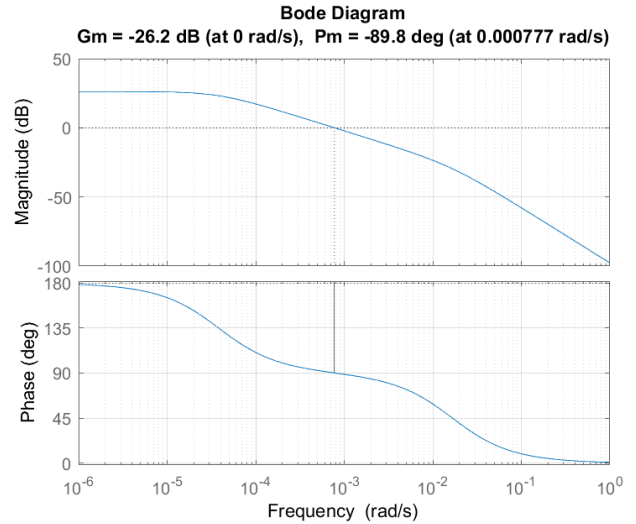


Fig. 6. Open loop system Bode plot without PID control

Due to the negative amplitude of the transfer function, the phase started at 180 degrees. The two poles each lowered the phase by 90 degrees and resulted in a phase of 0 degree at high frequencies. The gain margin of the system was -26.2 dB at 0 rad/s because at 0 rad/s, the phase was at an unstable 180 degrees, but the gain was 26.2 dB over 0 dB. The negative gain margin caused the system to be unstable at low frequencies around 0 dB. To make the system stable, we aimed for a gain margin of 10 dB. To achieve that, the overall magnitude should be lowered by  $26.2 + 10 = 36.2$  dB. Therefore,  $K_p = 10^{(-36.2/20)} = 0.0156$ . Though the system was now stable, the two poles resulted in a second order response, causing unwanted oscillations. Derivative control was used to make the system single order; the zero of derivative control canceled one pole of the system. The smaller pole at  $3.8303 \times 10^{-5}$  rad/s lowered the phase quickly at low frequencies and shifted the phase away from the unstable 180 degrees for all frequencies larger than it. Hence, the goal was to keep this pole and cancel the larger pole at 0.0167 rad/s. To do this, we set  $K_p/K_d = 0.0167$ . Plugging in  $K_p = 0.0156$ , the result is  $K_d = K_p/0.0167 = 0.9336$ . Since the system was already having a higher gain at low frequencies, the use of integral control would not enhance system performance significantly. Moreover, the pole and zero of integral control would make the change in phase and magnitude more complex and create more unwanted oscillations. Hence, we set  $K_i = 0$ .

## III. RESULTS

#### A. Bode Diagram

A bode diagram of the system's response, after PID was applied, was analyzed in order to quantify the system's stability. After lowering the gain to a positive gain margin of 10dB (using  $K_p = 0.0156$ ) and using derivative control to cancel pole  $1 = 0.0167$  (using  $K_d = 0.9336$ ), the frequency response in the bode diagram below predicts a single order system with less oscillations than in Fig. 6 above.

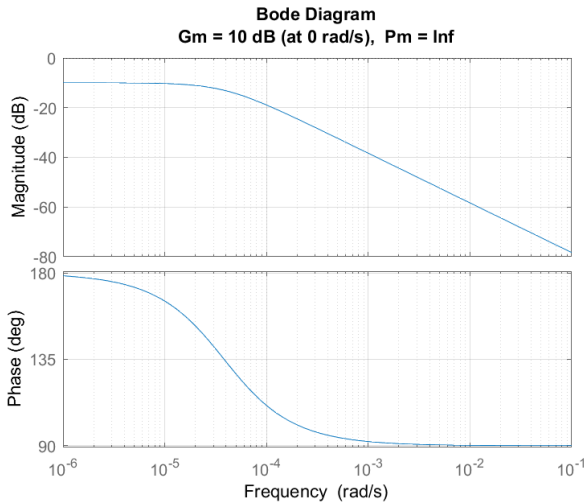


Fig. 7. This Bode Diagram predicts a stable system with the use of PID.

According to the behavior of the frequency response above, the system is presumed to act like a low pass filter. This now stable system, evidenced by its positive phase margin, is a considerable improvement compared to the unstable system results at steady state that the previous bode plot predicted without PID.

#### B. Errors in Simulation

The PID control aspect of the system was based on the idea that the ideal system would behave like a low pass filter. This determined the gain value which in turn helped derive the PID parameters. The system was successful in behaving how we intended it to, however more analysis could have been implemented in determining the ideal gain values that would further improve the system to reflect true physiological responses.

#### C. Simulation vs. Physiological Observations (9)

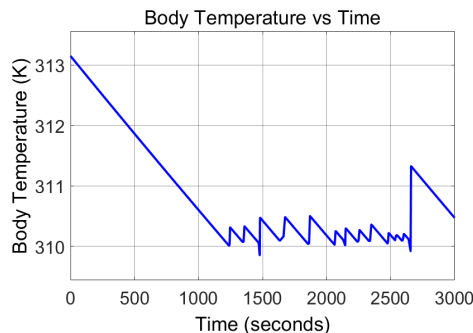


Fig. 7. Simulink simulation of Body Temperature over Time without PID control.

The results in this figure are consistent with the prediction that the system would be unstable at steady state without PID controls as seen in the Fig. 6 Bode Diagram results.

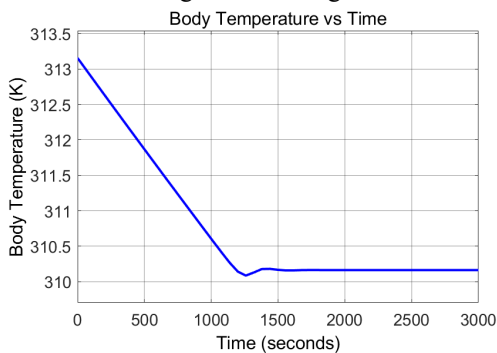


Fig. 7. Simulink simulation of Body Temperature over Time including only P control: ( $K_p = 0.0156$ ).

The system displays some oscillation in this plot seeing as it is a second order system with two poles. The system seems

to oscillate between 310.2K and 310.1K at 1385.029s and 1256.089s respectively.

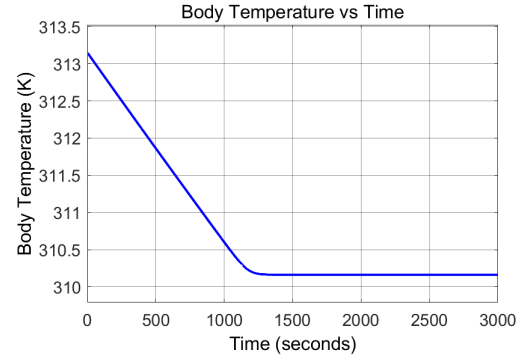


Fig. 10. Simulink simulation of Body Temperature over Time with PI control, where  $K_p = 0.0156$  and  $K_d = 0.9336$ .

Here, no oscillation is observed because  $K_d$  cancels one pole which converts the system into a single order system.

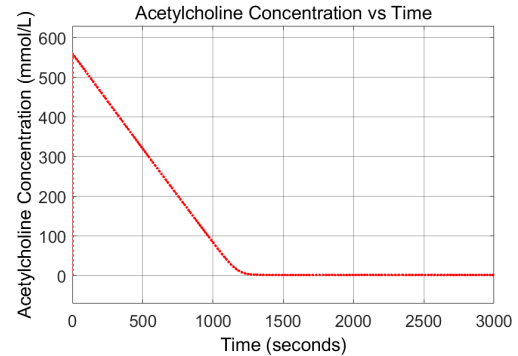


Fig. 11. Acetylcholine Concentration over Time with PID control.

The simulated behavior of the system makes sense in that the trend of a decreasing body temperature over time was correlated to the increase of acetylcholine concentration over time. The highest acetylcholine concentration occurs at the beginning of the hyperthermic simulation which correlates to the highest body temperature (ie. 313.15K). Fig. 11 displays a very similar pattern to Fig. 10 suggesting a correlation between acetylcholine concentration and body temperature. This supported the notion that the acetylcholine release in the body aided the cooling of the body under extreme conditions such as hyperthermia. The addition of PID control resulted in a stable, low pass filter system that successfully lowered the body temperature with a lack of oscillations in under an hour.

Although the control system performed as expected, there were some disparities to note between the simulink simulations and the reality in the physiological system. An important aspect in a real physiological response to hyperthermia is the vasodilation that helps cool the body in instances of hyperthermia. Because this system design fails to incorporate this natural mechanism, its results are likely inaccurate in this aspect as vasodilation would aid cool the body faster than the acetylcholine release mechanism alone. Should vasodilation be included in the system, the body temperature might have lowered faster over time in Fig. 8 and Fig. 9. Additionally, the acetylcholine concentration might have been lower than in Fig. 10 as less sweating might have been needed when it is combined with vasodilation. Another aspect that was simplified to a constant in this system was metabolic rate where in reality it would likely increase in the case of hyperthermia. This is another physiological reality that, if incorporated into this system, would likely cause a decrease in the acetylcholine concentration in Fig. 10 as the body

wouldn't depend on it as the only mechanism to lower the body's temperature [5][6]. The differences in the results in the system compared to the expected results of a real physiological system are due to the assumptions and simplifications that were made to facilitate the design and make the development of this system possible.

### III. DISCUSSION

#### A. Modified System

As neurotransmitter control of thermoregulation depends on afferent signals from skin thermoreceptors and efferent signals from the preoptic hypothalamus, disruption of this signaling pathway can result in modified system behavior. For instance, pathologies or disorders that affect the cholinergic nerves in the brainstem or spinal cord may disrupt the acetylcholine pathway for controlling sweat rate. Based on existing literature, patients with spinal cord injury (SCI), such as with high-level thoracic spinal cord lesions, have exhibited lower whole-body sweat rates and cooling potential than able-bodied individuals. Regression lines comparing whole-body sweat rates between SCI and able-bodied athletes indicated an approximate 50% decrease in  $S_{rate}$  for the former [7]. Hence, the risk of heat injuries increased; while the system remains a stable first order system, the time taken to return to target body temperature is increased. To simulate this type of disease, a gain of 0.5 was applied to the sweat rate in the Simulink model shown below to reduce the whole-body sweat rates by a half.

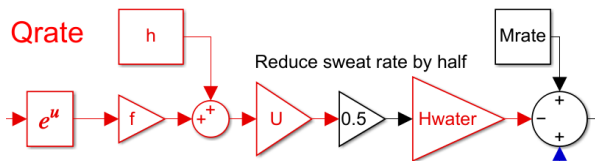


Fig. 12. Modified section of Simulink model for simulating the effects of decreased sweat rate

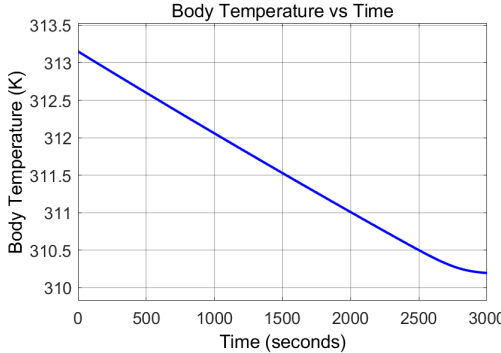


Fig. 13. Body temperature vs time pathological model for SCI patients

#### B. Clinical Application

The model has several advantages. Due to the simplicity of only considering one active method for the body to lower the temperature by releasing of acetylcholine and the corresponding increase in sweat rate, and some easily adjustable parameters for each individual such as body mass and body surface area, the effectiveness of how a certain amount of acetylcholine lowers the body temperature for different patient can be quickly approximated. The time for patients under hyperthermia to return to normal body temperature through sweating, and the amount of water loss due to that sweating can also be estimated. This can potentially provide quick information for treatments such as how much water should be supplied to a patient under hyperthermia to help the patient return to normal condition. The model can also

help understand how the ability of body temperature regulation may be negatively affected in patients who have abnormal regulation of acetylcholine concentration owing to diseases like Alzheimer's, Parkinson's and Huntington [8], and it can also be applied to sweat rate related diseases such as pathologies or disorders in cholinergic nerves that were previously mentioned. The mathematical relationships between acetylcholine concentration and sweat rate developed can also serve as a blueprint for developing a more accurate mathematical model. The limitations of the model are also caused by its simplicity and assumptions made. The model does not consider other important active approaches for the body to regulate temperature such as vasoconstriction and vasodilation. It also does not consider other hormones or neurotransmitters that play important roles in body temperature regulation such as norepinephrine that causes significant vasoconstriction that leads to rise in body temperature [9]. Moreover, the metabolic rate is held constant, which will not be a good approximation for people that are under high intensity motions. Furthermore, the math model describes sweat rate and acetylcholine concentration may not apply to every individual. Further research is needed to form a more accurate, individual-based model.

#### ACKNOWLEDGEMENTS

We would like to thank Professor Cauwenberghs and TAs Becky Chin and Will Sharpless for their time and efforts in assisting us throughout the quarter on BENG 122A's subject material and for offering feedback on our project.

#### REFERENCES

- [1] Tata, A. M., Velluto, L., D'Angelo, C., & Reale, M. (2014). Cholinergic system dysfunction and neurodegenerative diseases: cause or effect?. *CNS & neurological disorders drug targets*, 13(7), 1294–1303. <https://doi.org/10.2174/1871527313666140917121132>
- [2] Sharma, Ragav. and Sandeep Sharma. "Physiology, Blood Volume." *StatPearls*, StatPearls Publishing, 14 April 2022.
- [3] Kofke, W. Andrew, et al. "Middle Cerebral Artery Blood Flow Velocity and Stable Xenon-Enhanced Computed Tomographic Blood Flow during Balloon Test Occlusion of the Internal Carotid Artery." *Stroke*, vol. 26, no. 9, 1 Sept. 1995, pp. 1603–1606., <https://doi.org/10.1161/01.str.26.9.1603>.
- [4] Sacco, Joseph J., et al. "The Average Body Surface Area of Adult Cancer Patients in the UK: A Multicentre Retrospective Study." *PLoS ONE*, vol. 5, no. 1, 28 Jan. 2010, <https://doi.org/10.1371/journal.pone.0008933>.
- [5] Xu, Xiaojiang, et al. "The Specific Heat of the Human Body Is Lower than Previously Believed: The Journal Temperature Toolbox." *Temperature*, 22 July 2022, pp. 1–5., <https://doi.org/10.1080/23328940.2022.2088034>.
- [6] Bhatia, Dinesh, and Urvashi Malhotra. "Thermophysiological Wear Comfort of Clothing: An Overview." *Journal of Textile Science & Engineering*, vol. 06, no. 02, 21 Apr. 2016, <https://doi.org/10.4172/2165-8064.1000250>.
- [7] Price, M.J. Thermoregulation during Exercise in Individuals with Spinal Cord Injuries. *Sports Med* 36, 863–879 (2006). <https://doi.org/10.2165/00007256-200636100-00005>.
- [8] de Dear, R., Arens, E., Hui, Z. et al. Convective and radiative heat transfer coefficients for individual human body segments. *Int J Biometeorol* 40, 141–156 (1997). <https://doi.org/10.1007/s004840050035>.
- [9] Hjemdal, P et al. "Vascular and metabolic effects of circulating epinephrine and norepinephrine. Concentration-effect study in dogs." *The Journal of clinical investigation* vol. 64,5 (1979): 1221-8. doi:10.1172/JCI109576